

1. ABSTRACT

Simulating intervals such as the Permian Triassic Mass Extinction that are potentially exacerbated by climate system feedbacks is crucial for validating future climate predictions under heightened greenhouse gas levels, during transitions to hothouse conditions. Here, we develop and prescribe boundary conditions consistent with the reconstructed topography at 1°x1° resolution for the CESM1.3 model for model intercomparison projects. Sensitivity experiments forced with these boundary conditions and various CO2 levels, relative to present-atmospheric levels of 280 ppmv, and aerosol loadings (using BAM) can resolve the competing effects of greenhouse warming and aerosol induced increases in cloud-optical thickness and cooling. In this study we aim to derive the estimates for the global mean surface temperature (GMST) from the most recent, high-resolution datasets for selective locations of interest for synthesis with the GMSTs derived from the modeled data to quantify the climate sensitivity. Such synthesis can provide valuable insights into how Earth's climate responded to extreme warming events in the past and how it might respond under similar conditions in the future as well as bridging the gap for quantifying climate feedbacks leading to the largest biotic crisis in the geologic past.

2. INTRODUCTION

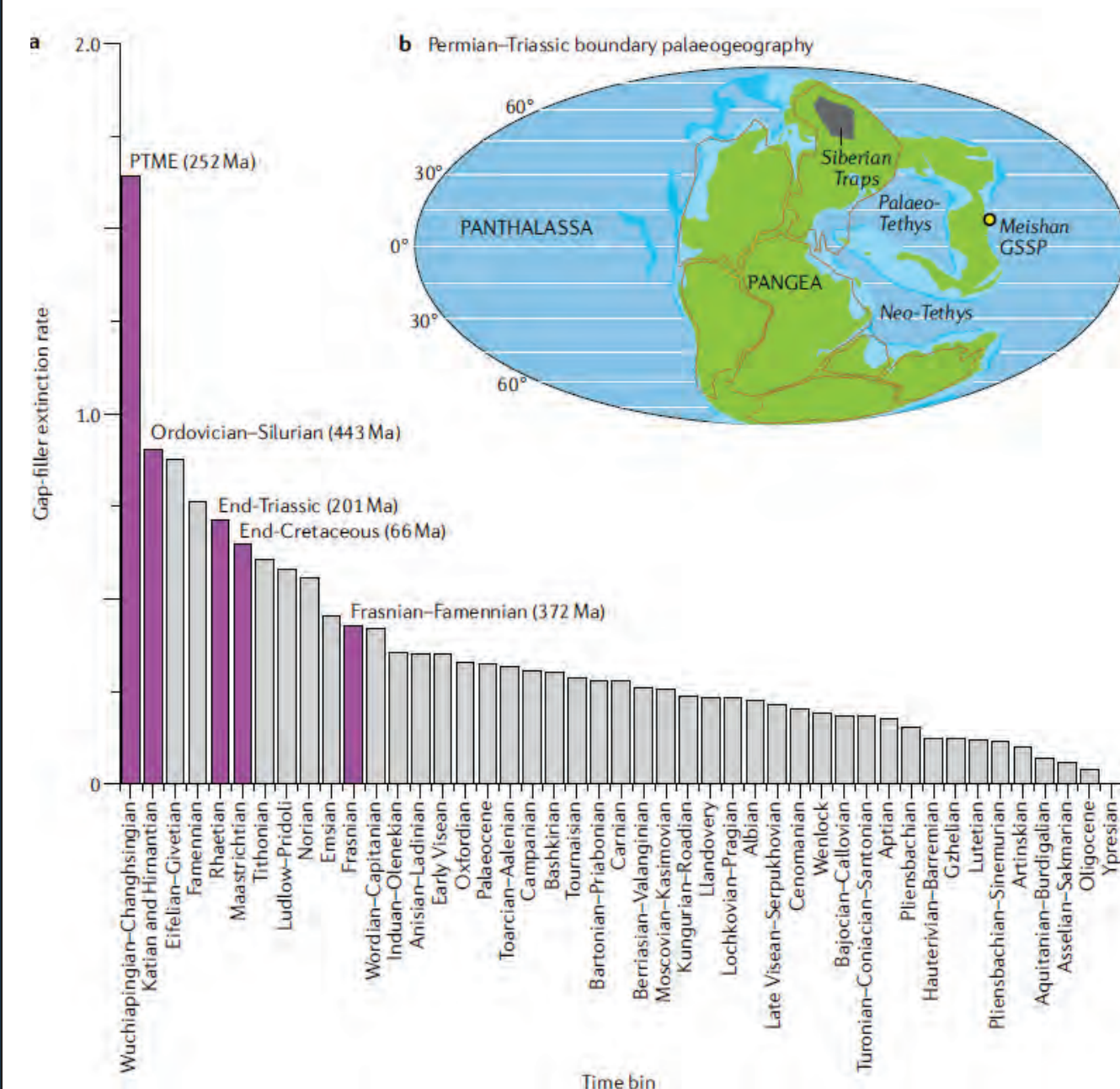


Figure 1. PTME extinction and its world (Corso et al., 2022)

- PT mass extinction occurred ~251.9 Ma (Payne and Clapham, 2012)
- Around 81%-94% of marine and 70% of terrestrial species went extinct (Corso et al., 2022)

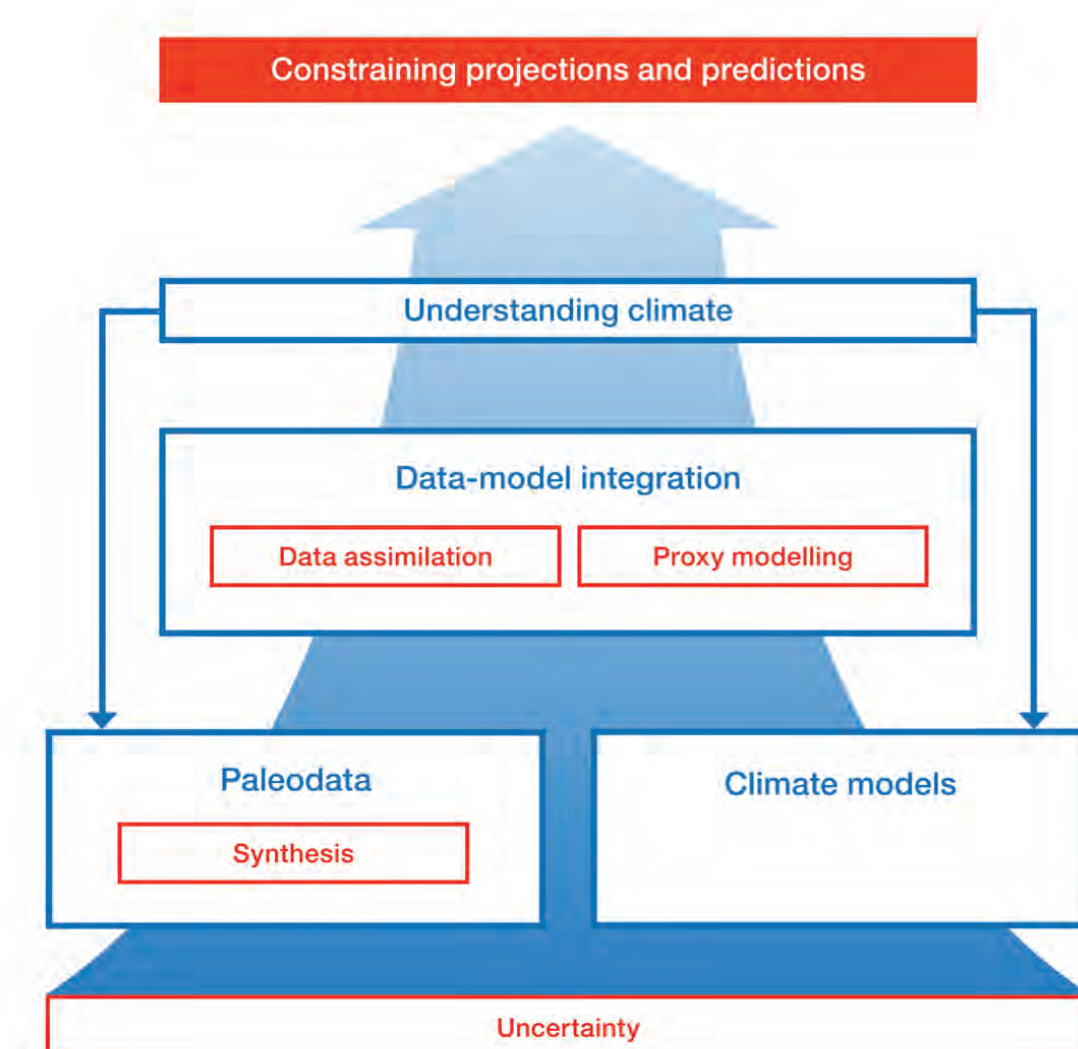


Figure 2. Schematic workflow of paleo proxy-model data integration to improve and constrain the understanding of climate system. The three main challenges are highlighted in red that need to be addressed to constrain the uncertainty related to the paleoclimate models as well as data (Jonkers et al. 2021).

3. METHODOLOGY

Atmosphere 1.9° x 2.5° | Ocean 1° x 1°

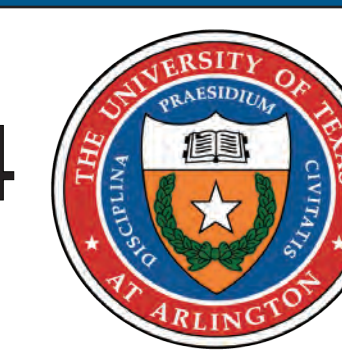
Figure 3. CESM1.3 Model Description (National Center for Atmospheric Research, NCAR)

Table 1. Prescribed Solar Insolation (S₀) and Orbital Parameters for CESM1.3 (Kiehl and Shields, 2005; Winguth et al., 2015)

S ₀ (W/m ²)	Eccentricity	Obliquity
1338	280	0.700



Discover 2024



Hothouse Climate Modeling During the Late Permian-Early Triassic Interval using CESM1.3 With An Emphasis On Model-Data Comparisons

-Gautam M¹., Winguth A¹., Winguth C¹., Scotese C²., Osen A³

¹University of Texas at Arlington, TX; ²Northwestern University, IL; ³Tarrant County Community College, TX

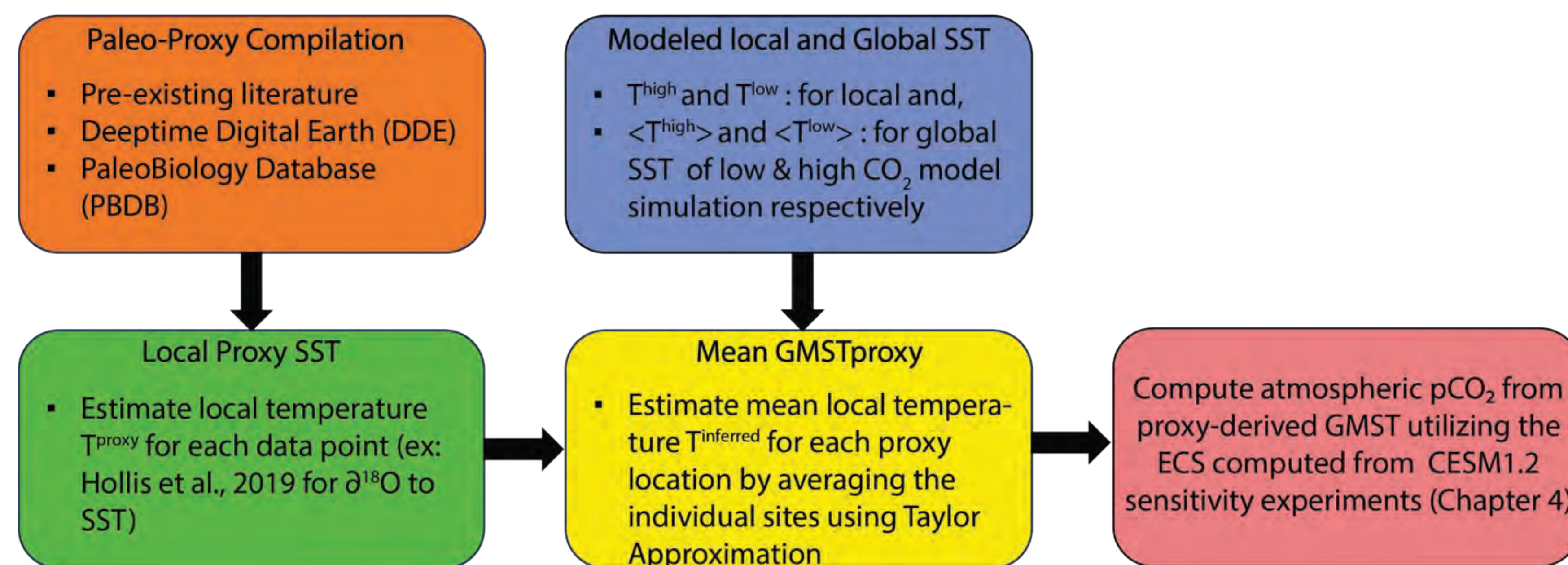


Figure 4. Overall methodology for data-model synthesis as adopted from Inglis et al. (2020). The resulting GMST will be independent of the model climate sensitivity but dependent on modeled spatial distribution of temperature.

- Estimation of Global Proxy SST follow Fransworth et al., (2019) as mentioned in Inglis et al., (2020) as follows:

$$\langle T_{inferred} \rangle = \langle T^{low} \rangle + (T_{proxy} - T^{low}) \frac{\langle T^{high} \rangle - \langle T^{low} \rangle}{T^{high} - T^{low}}$$

$\langle T^{high} \rangle$ and $\langle T^{low} \rangle$ are global means of high- and low- CO₂ simulation, respectively, $T^{high} - T^{low}$ are the local Land Air Temperatures for the respective model simulation scenarios and T_{proxy} is the proxy temperature estimate.

4. PRELIMINARY RESULTS

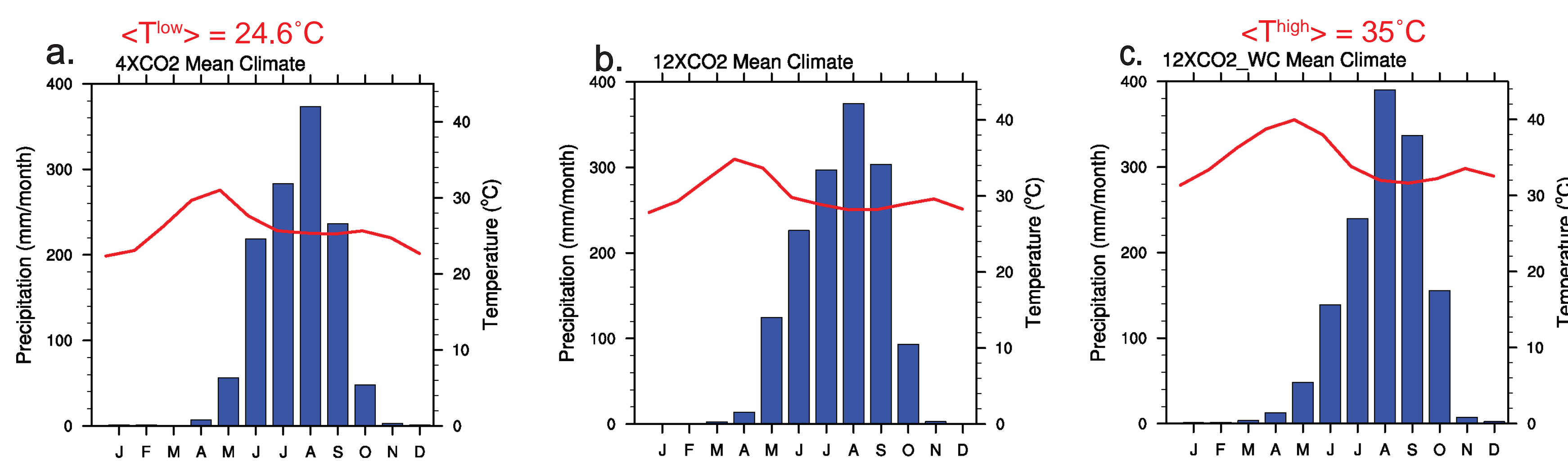


Figure 5. Climatology graphs for North China (21°N 107°E) from CCSM3 model results for Permian-Triassic interval. The three panels show the various sensitivity experiments for CO₂ radiative forcings relative to PAL of 280ppm with a) 4x CO₂, b) 12x CO₂ as well as c) 12x CO₂ with thin cloud cover.

Table 2. Soil temperatures for the various paleo-proxy locations and their respective temperature estimates (Courtesy of Joachimski et al., 2022).

Pale-proxy location	Paleolatitude	Late Permian °C	Early Triassic °C
Xinjiang	45° N	15 - 25	25 - 35
Russia	30-35° N	15 - 25	25 - 35
North China	20° N	20 - 30	30 - 40
Karoo	55-60° S	15 - 25	25 - 35
Low latitude SST		26	35

Note: they used a ± 5° C temperature range around calculated average soil temperature for pCO₂ calculations.

5. DISCUSSION AND FUTURE WORK

- The mean proxy-inferred temperature LAT for North China is 23°C.
- Similar to this step, once the LAT(inferred)is calculated for rest of the paleo-locations, the GMST will be calculated using the global scaling factor.
- The pCO₂ from proxy-derived GMST utilizing the ECS computed from CESM1.3 sensitivity experiments.
- Such point-to-point model-proxy synthesis will allow for better constraints on the pCO₂ estimates which still exist in a vastly proposed range.
- This will also allow to address any missing feedbacks that could be evaluated to simulate such climate transitions into a hothouse world.

6. REFERENCES

Dal Corso, J. et al. Permo-Triassic boundary carbon and mercury cycling linked to terrestrial ecosystem collapse. Nature communications 11, 2962 (2022).

Farnsworth, A., Lunt, D., O'Brien, C., Foster, G., Inglis, G., Markwick, P., Pancost, R., and Robinson, S.: Climate sensitivity on geological timescales controlled by non-linear feedbacks and ocean circulation. Geophysical Research Letters (46), 9880-9889 (2019).

Inglis, G.N., Bragg, F., Burls, N.J., Cramwinckel, M.J., Evans, D., Foster, G.L., Huber, M., Lunt, D.J., Siler, N., Steinig, S. and Tierney, J.E. Global mean surface temperature and climate sensitivity of the early Eocene Climatic Optimum (EECO), Paleocene-Eocene Thermal Maximum (PETM), and latest Paleocene. Climate of the Past 16(5), 1953-1968, (2020).

Jonkers, L., Bothe, O. and Kucera, M. Preface: Advances in paleoclimate data synthesis and analysis of associated uncertainty: towards data-model integration to understand the climate. Climate of the Past, 17(6), 2577-2581 (2021).

Joachimski, M., Müller, J., Gallagher, T., Matthes, G., Chu, D., Mouraviev, F., Silantiev, V., Sun, Y. and Tong, J. Atmospheric CO₂ history of the late Permian and Early Triassic (No. EGU23-9038). Copernicus Meetings, (2022).

Kiehl, J.T. and Shields, C.A. Climate simulation of the latest Permian: Implications for mass extinction. Geology, 33(9), 757-760 (2005).

Lunt, D.J., Bragg, F., Chan, W.L., Hutchinson, D.K., Ladant, J.B., Niezgodzki, I., Steinig, S., Zhang, Z., Zhu, J., Abe-Ouchi, A. and de Boer, A.M. DeepMIP: Model intercomparison of early Eocene climatic optimum (EECO) large-scale climate features and comparison with proxy data. Climate of the Past Discussions, 21-27, (2020).

Payne, J.L., and Clapham, M.E. End-Permian mass extinction in the oceans: An ancient analog for the twenty-first century?: Annual Review of Earth and Planetary Sciences, 40(1), 89-111 (2012).

Winguth, A.M., Shields, C.A. and Winguth, C. Transition into a hothouse world at the Permian-Triassic boundary—a model study. Palaeogeography, Palaeoclimatology, Palaeoecology 440, 316-327 (2015).

ACKNOWLEDGEMENTS

We would like to acknowledge the National Science Foundation for their continued support of this project through both NSF grants EAR 1636629. Without their support, these projects and experiments would not have been possible.

In addition, we would like to thank the National Center for Atmospheric Research for their technical support with developing and cultivating these model simulations.

All model simulations are currently being carried out on NCAR Wyoming Super Computing Center, which is supported by NSF.